Research Article | Vol. 27, No. 22 / 28 October 2019 / Optics Express 31773
Optics EXPRESS

Ring-core few-mode fiber for tunable true time delay line operation

SERGI GARCÍA,* RUBÉN GUILLEM, AND IVANA GASULLA

ITEAM Research Institute, Universitat Politècnica de València, Camino de Vera, 46022 Valencia, Spain
*sergarc3@iteam.upv.es

Abstract: We propose, for the first time to our knowledge, tunable true time delay line operation for radiofrequency signals on a few-mode fiber link. In particular, the custom design of a 7-LP-mode ring-core few-mode fiber together with a set of 5 broadband long period gratings inscribed at the proper positions along the fiber allows 4-sample true time delay line tunability over a 20-nm optical wavelength range. We study the performance of the designed true time delay line in the context of reconfigurable microwave photonics signal processing by theoretically evaluating microwave signal filtering and optical beamforming networks for phased array antennas.

1. Introduction

Although space-division multiplexing (SDM) technologies emerged as a solution to the upcoming transmission capacity bottleneck in optical fiber networks [1], they are gathering an increasing interest in other applications beyond high-capacity digital communications, such as multi-parameter optical fiber sensing [2] and radiofrequency (RF) signal processing [3].

Recently, we have demonstrated the potential of different SDM optical fibers to implement what we coined as "fiber-distributed signal processing", where the data signal is processed while it is distributed through the optical fiber, [3]. The idea is to exploit the inherent parallelism of a single SDM optical fiber to implement a compact and efficient approach for sampled true time delay line (TTDL) operation, which is actually the basis of discrete-time incoherent signal processing, [4]. The goal of a TTDL is to provide a set of time-delayed samples of the RF signal with tunable group delays within a given RF frequency range. Different approaches have been reported for the implementation of true time delay lines over the past 30 years, where the required diversity is realized by exploiting either the time or the wavelength multiplexing domains. Tunable configurations built upon single-core singlemode fibers include switched fibers [5], dispersive fibers [6], Fiber Bragg Grating (FBG) inscription [7] and exploitation of nonlinearities such as Stimulated Brillouin Scattering [8].

Time delay line operation is of special interest in the context of next-generation fiber-wireless communications systems, such as 5G radio access networks and the Internet of Things, which demand a variety of microwave photonics (MWP) signal processing functionalities, including signal filtering, optical beamforming for phased-array antennas and arbitrary waveform generation [9]. In this sense, we foresee that MWP signal processing and radio-over-fiber distribution can benefit greatly from the use of different SDM fiber technologies in terms of compactness and weight, while assuring broadband versatility and reconfigurability. This brings a relevant challenge that involves the development of novel multicore fiber (MCF) [10,11] or few-mode fiber (FMF) [12,13] solutions where the different spatial paths (cores or modes) provide the required time-delayed signal samples.

Figure 1 shows the general rationale behind the implementation of a tunable TTDL for RF signals with an FMF. The goal is to obtain at the output of the fiber link, a set of time-delayed replicas of the modulated signal assuring a constant differential delay between adjacent replicas (named as basic differential delay, $\Delta\tau$) at a given optical wavelength [9]. We must ensure, in addition, a low level of coupling between non-degenerate modes, what calls in general for

#374367 https://doi.org/10.1364/OE.27.031773
Journal © 2019 Received 2 Aug 2019; revised 3 Oct 2019; accepted 10 Oct 2019; published 17 Oct 2019

Optics EXPRESS

refractive step-index (SI) profiles and the use of short distances combined with direct detection. We can say that the scheme illustrated in Fig. 1 corresponds to 1-dimensional (1D) operation since all the replicas result from exploiting the fiber spatial diversity (modes or groups of modes) inherent to the FMF. If we feed the TTDL by a multi-carrier optical source (instead of a single-carrier source), the same fiber link will offer 2-dimensional (2D) operation since we can exploit, in addition to the spatial diversity, the optical wavelength diversity, [2].

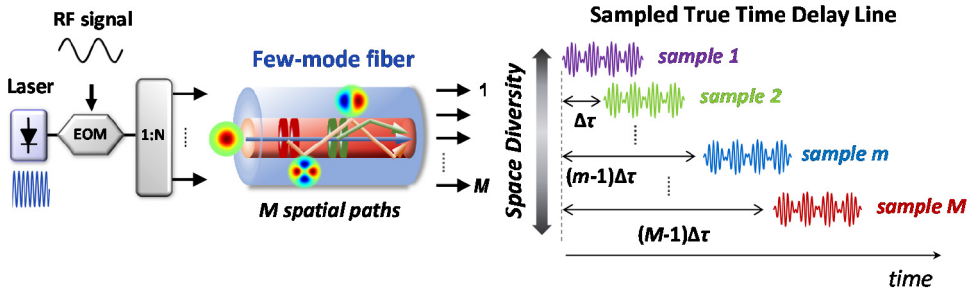

Fig. 1. Tunable true time delay line based on an FMF with the inscription of LPGs.

We have previously reported different solutions for FMF-based TTDLs that work only in the 1D diversity regime by exploiting the spatial diversity at a single optical wavelength, [12,13]. In [12], we experimentally demonstrated 3-sampled TTDL operation on a 60-m SI 4-LP-mode fiber where 3 LP modes were injected at the fiber input and a long period grating (LPG) was inscribed to generate and adjust the time delay of the sample associated to the LP_{02} mode. Two different configurations (with different basic differential delays) were implemented on the same FMF-based device by selecting a different set of 3 modes at the fiber output for a particular optical wavelength of 1558.3 nm. That idea was improved in a latter work [13], where we experimentally demonstrated 4-sampled TTDL operation on a 44.4-m link of the same SI 4-LP-mode fiber. There, the inscription of a set of LPGs at specific locations along the fiber allowed the excitation of the 3 higher-order modes while adjusting the individual sample group delays and amplitudes. Since one requires only to inject the fundamental mode, this second approach is independent of any preceding additional fiber link that may be required to distribute the signal. However, as it happened in [12], that TTDL only works properly for a single optical wavelength around 1558 nm and does not allow continuous tunability with an external parameter such as the optical wavelength.

In the general context of MWP signal processing, it is desirable to have the capability to tune the basic differential delay so we can reconfigure our target application (changing, for instance, the free spectral range of a signal filter or the beam-pointing angle of a phased array antenna). This means that the basic differential delay must vary linearly with the optical wavelength. In other words, we need different values of the chromatic dispersion (spectral group delay slopes) associated to each sample.

With this aim in mind, we propose here an FMF-based 4-sample TTDL approach that offers, for the first time to our knowledge in the context of FMFs, time delay tunability over a given optical wavelength range. This solution combines the custom design of a 7-LP-mode ring-core fiber and the inscription of 5 LPGs at the appropriate locations along the FMF to achieve both constant differential time delay and differential chromatic dispersion values between the TTDL signal samples. Section 2 proposes the concept for tunable TTDL in an FMF link with inscribed LPGs, while section 3 describes the specific design of both the FMF and the LPGs to be inscribed. In section 4, we theoretically evaluate the proposed TTDL in the context of reconfigurable microwave signal filtering and radio beam-steering in phased array antennas. Finally, section 5 closes the paper with the relevant conclusions and future directions of research.

Optics EXPRESS

2. Few-mode fiber tunable true time delay line concept

The use of sampled TTDLs for time-discrete signal processing implies that the differential delay between adjacent samples, i.e. the basic differential delay $\Delta\tau$, must be constant for all the samples at a given optical wavelength. Time-delay tunability with the wavelength implies in addition, a linear increment of this basic differential delay with the optical wavelength. In the particular case of an FMF-based TTDL, if we exploit the space-diversity domain, the samples correspond to different modes (or groups of modes) that propagate along the fiber for a given wavelength. If we use wavelength diversity instead, the samples are given by the different optical wavelengths carried by a given mode (or group of modes).

We can expand the group delay per unit length of a given LP_{lm} mode, τ_{lm}, in 1st-order Taylor series around a central or reference wavelength λ_0 as

$$\tau_{lm}(\lambda) = \tau_{lm}(\lambda_0) + (\lambda - \lambda_0)D_{lm}, \tag{1}$$

where $\tau_{lm}(\lambda_0)$ is the group delay per unit length at λ_0 and D_{lm} is the chromatic dispersion at λ_0 for the LP_{lm} mode. TTDL tunability with the wavelength requires the set of parameters D_{lm} to follow as well an incremental law with a constant increment between adjacent samples ΔD, [3]. This way, the basic differential delay when we operate in the spatial diversity domain can be expressed as:

$$\Delta\tau(\lambda) = \Delta\tau(\lambda_0) + (\lambda - \lambda_0)\Delta D. \tag{2}$$

All in all, two conditions must be satisfied in Eq. (2) for proper TTDL operation and tunability: (1) constant basic differential group delay at the central wavelength $\Delta\tau(\lambda_0)$; and (2) constant basic differential chromatic dispersion ΔD. In general, it is not possible to fulfil these conditions given the propagation characteristics of the modes that propagate through typical FMFs. And, even in the hypothetical case that it was possible, the differential group delay $\Delta\tau$ would probably be extremely high for MWP applications, (i.e., very low operating radio frequencies), limiting the fiber length to only a few meters. In addition, the contribution corresponding to the differential group delay at the reference wavelength $\Delta\tau(\lambda_0)$ would be much greater than the contribution corresponding to the incremental dispersion $(\lambda\text{-}\lambda_0)\Delta D$ in Eq. (2), so that the TTDL tunability would be insignificant.

To overcome these limitations, we propose to obtain a subset of TTDL samples as a combination of different modes that propagate through the fiber instead of using a single mode per sample. With the help of in-line mode converters based on LPGs inscribed at specific positions along the FMF link [14], we can adjust the final group delay and chromatic dispersion values associated to each signal sample. This idea can be explained as follows. Suppose that the i^{th} TTDL sample is created in first place by a particular mode LP_{lm} that is injected at the fiber input and propagates over that mode for a certain distance $L_{lm}{}^{(i)} = l_{lm}{}^{(i)}L$ (with a specific group delay and chromatic dispersion), where $l_{lm}{}^{(i)}$ is the normalized length along which the i^{th} sample is propagated by a given LP_{lm} mode and L is the total length of the FMF link. Then, a given LPG transforms that incoming LP_{lm} mode into a different outgoing LP_{lm} mode (with a different group delay and chromatic dispersion). We can repeat this mode conversion mechanism as many times as necessary by concatenating different LPGs inscribed at the positions $\sum_{lm\in I} l_{lm}{}^{(i)}L$, where I is the set of indices lm of the LP_{lm} modes in which the i^{th} sample has been propagated before passing through the current LPG. This way, at the output of the fiber, the group delay of the i^{th} TTDL sample τ_i at a given wavelength λ_0 can be expressed as a combination of the LP_{lm} modes involved to create that sample as

$$\tau_i = \left[\left(\sum_{lm\in I}\tau_{g,lm}l_{lm}^{(i)}\right) + (\lambda - \lambda_0)\left(\sum_{lm\in I}D_{lm}l_{lm}^{(i)}\right)\right]L = [\tau_{eq,i} + (\lambda - \lambda_0)D_{eq,i}]L, \tag{3}$$

Optics EXPRESS

where $\tau_{eq,i}$ and $D_{eq,i}$ are the equivalent group delay per unit length and equivalent chromatic dispersion of the i^{th} sample at λ_0, respectively. With the appropriate mode combination, we can assure a set of samples with constant incremental group delay and dispersion values between adjacent samples, given by

$$\tau_i = \tau_{eq,1}L + (i-1)\Delta\tau(\lambda_0) + (\lambda - \lambda_0)(D_{eq,1} + (i-1)\Delta D)L, \tag{4}$$

where $\tau_{eq,1}$ is the equivalent group delay per unit length of the first sample and $D_{eq,1}$ is the equivalent chromatic dispersion of the first sample. Figure 2 illustrates the basic idea beyond the mode combination mechanism in Eqs. (3) and (4) for a generic FMF link with inscribed LPGs. Figure 2(a) shows the evolution of the differential group delay of the samples, $\tau_i - \tau_1$, at the anchor wavelength λ_0, as a function of the normalized length z/L. Each colored line corresponds to a different mode of a generic FMF. We see that proper mode conversion in samples 2 and M allows the common basic differential delay requirement, $\Delta\tau(\lambda_0)$. In a similar way, Fig. 2(b) depicts the evolution of the sample differential chromatic dispersions, $D_i - D_1$, as a function of the normalized length, where we see that one can obtain as well incremental values of the chromatic dispersion with a common differential dispersion, ΔD. Finally, Fig. 3(c) represents the dependence of the resulting sample time delays with the optical wavelength, where we can observe the tunability of the TTDL with the optical wavelength.

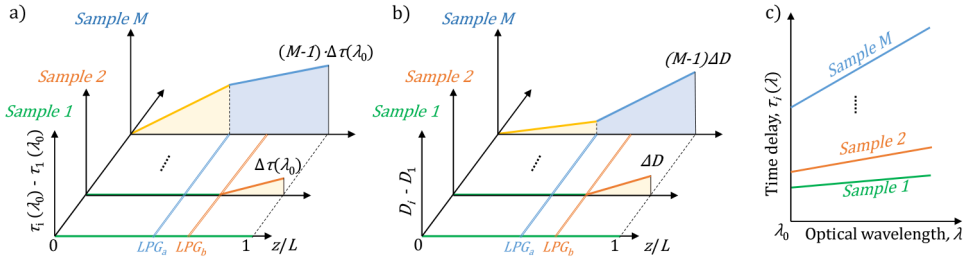

Fig. 2. (a) Evolution of the differential group delay of the samples, $\tau_i - \tau_1$, as a function of the normalized length; (b) Evolution of the differential chromatic dispersion, $D_i - D_1$, as a function of the normalized length; and (c) Time-delay dependence of the samples with the optical wavelength for a generic FMF link with inscribed LPGs.

3. Design of true time delay line on a 7-mode fiber

We have described in the previous section the conditions that the FMF-based device must fulfil to operate as a sampled TTDL. But we need to ensure as well a low level of intermodal crosstalk between signal samples along the fiber link to avoid degradation on the target MWP signal processing functionality, what calls for modal phase propagation constants (or effective indices) as different as possible. In addition, modes with a set of chromatic dispersions as diverse as possible are desirable to allow the accomplishment of Eq. (3) with higher ΔD (larger delay tunability). In this regard, we have designed a particular FMF whose refractive index profile follows a ring-core step-index architecture. The use of a step-index profile reduces the mode coupling by increasing the effective index difference between modes, while the ring-core architecture provides more design versatility and allows to manage the propagation characteristics of the symmetric modes with certain independence from the asymmetric modes. Figure 3(a) depicts the refractive index profile of the designed ring-core fiber. It consists of a SiO_2 inner layer doped with a low GeO_2 concentration (radius $a_1 = 3\,\mu$m and inner-core-to-cladding relative index difference $\Delta_1 = 0.21\%$) surrounded by a SiO_2 ring-core layer doped with a higher GeO_2 concentration (radius $a_2 = 10\,\mu$m and core-to-cladding relative index difference $\Delta_2 = 0.72\%$) inside a pure silica

Optics EXPRESS

cladding. Figure 3(b) shows the computed effective index as a function of the scale factor (i.e., the parameter that expands/compacts the whole refractive index profile in the radial axis r). When the scale factor equals 1, the refractive index profile corresponds to the designed profile. At this point, the fiber supports 7 LP modes. Table 1 summarizes the main characteristics of the fiber modes at a 1550-nm wavelength.

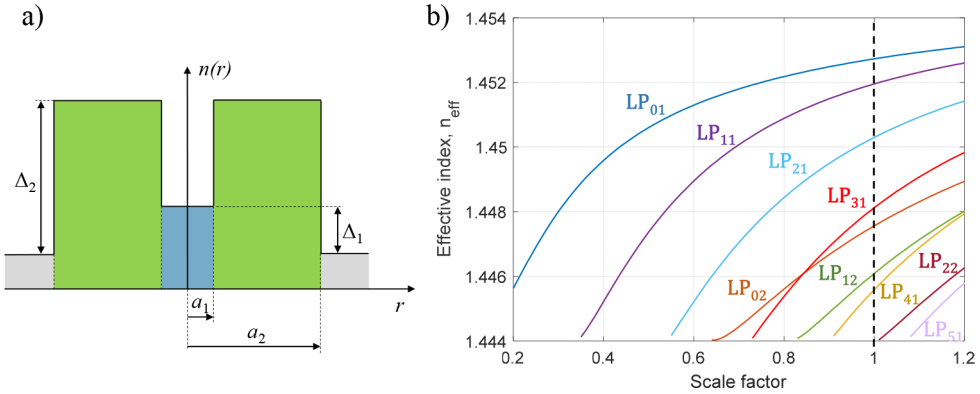

Fig. 3. (a) Refractive index profile of the designed ring-core fiber. (b) Computed effective index n_{eff} for every propagated mode as a function of the fiber scale factor.

Table 1. Propagation characteristics of the modes for the designed FMF at $\lambda_0 = 1550$ nm.

	LP_{01}	LP_{11}	LP_{21}	LP_{31}	LP_{02}	LP_{12}	LP_{41}
$\tau_{lm} - \tau_{01}$ (ps/km)	0	3489.08	8182.33	13022.34	2858.64	8912.83	17412.05
D (ps/km/nm)	18.96	23.77	27.41	29.19	17.14	11.07	25.24
n_{eff}	1.452726	1.451956	1.450294	1.448120	1.447556	1.446090	1.445584

In order to reduce the crosstalk among non-degenerate modes, we have designed the fiber to increase as much as possible the effective index difference between the modes Δn_{eff} [15,16]. In this case, the effective index difference between neighboring modes is bigger than $0.5 \cdot 10^{-3}$ for all the modes, which is similar to the values of typical low-crosstalk commercial step-index FMFs. This is the case, for instance, of the FMF we reported in our previous articles for propagation of only 4 modes ($\Delta n_{eff} > 0.8 \cdot 10^{-3}$, ensuring low mode coupling below -30 dB/km) [12,13], where no significant distortions of TTDL performance were observed.

The evaluation of the modal propagation characteristics gathered in Table 1 suggests that a total of 5 LPGs acting as mode converters are required to perform 4-sample TTDL operation, that is, mode conversions: LP_{02} to LP_{12}, LP_{12} to LP_{01}, LP_{01} to LP_{41}, LP_{12} to LP_{11} and LP_{11} to LP_{31}. Figure 4 illustrates the designed ring-core fiber with the inscription of the LPGs along the fiber. We see there how the modes are combined through the different LPGs to generate the output samples. Starting from the 4th sample (the one with the largest group delay), we can see that it travels into the LP_{21} mode along the whole fiber length L. The remaining samples are created through LPG mode conversion, starting from the excitation of the LP_{02} mode at the fiber input. After a given length $L_{02} = l_{02} \cdot L$, LPG_1 couples all the power coming from this mode into the LP_{12} mode. After propagating through a length $L_{12}{}^{(1)} = l_{12}{}^{(1)} \cdot L$, the LP_{12} mode creates at the output of the fiber the 1st sample (the one with the smallest group delay). The group delay of the 2nd and 3rd samples is adjusted by performing two additional mode transformations in each case. For the 2nd sample, LPG_3 couples part of the LP_{12} mode into the LP_{01} mode that propagates a distance $L_{01}{}^{(2)} = l_{01}{}^{(2)} \cdot L$ before being transformed into the LP_{41} mode in LPG_5. In the case

Optics EXPRESS

of the 3rd sample, LPG_2 couples part of the LP_{12} mode into the LP_{11} mode that propagates a distance $L_{11}^{(3)} = l_{11}^{(3)} \cdot L$ before being transformed into the LP_{31} mode in LPG_4.

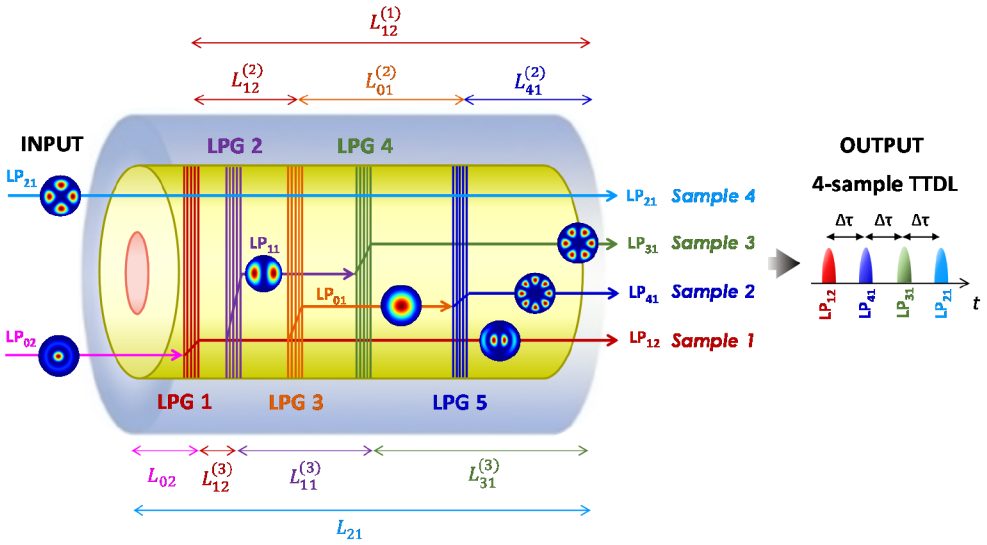

Fig. 4. Scheme of the designed TTDL based on a ring-core FMF link of length L with a set of 5 LPGs inscribed at specific longitudinal positions. On the right, one can see the 4 output TTDL samples in the time domain characterized by a constant basic differential delay $\Delta\tau$.

With the help of Eq. (3) and following the procedure illustrated in Fig. 4, we obtain the following expressions for the group delays per unit length of the samples at the end of the FMF link:

$$\begin{cases} \frac{\tau_1}{L} = (\tau_{02} l_{02} + \tau_{12} l_{12}^{(1)}) + (\lambda - \lambda_0)(D_{02} l_{02} + l_{12}^{(1)} D_{12}) \\ \frac{\tau_2}{L} = (\tau_{02} l_{02} + \tau_{12} l_{12}^{(2)} + \tau_{01} l_{01}^{(2)} + \tau_{41} l_{41}^{(2)}) + (\lambda - \lambda_0)(D_{02} l_{02} + D_{12} l_{12}^{(2)} + D_{01} l_{01}^{(2)} + D_{41} l_{41}^{(2)}) \\ \frac{\tau_3}{L} = (\tau_{02} l_{02} + \tau_{12} l_{12}^{(3)} + \tau_{11} l_{11}^{(3)} + \tau_{31} l_{31}^{(3)}) + (\lambda - \lambda_0)(D_{02} l_{02} + D_{12} l_{12}^{(3)} + D_{11} l_{11}^{(3)} + D_{31} l_{31}^{(3)}) \\ \frac{\tau_4}{L} = \tau_{21} l_{21}^{(4)} + (\lambda - \lambda_0) D_{21} l_{21}^{(4)} \end{cases}, \tag{5}$$

where the superscript of the normalized length $l_{02} = l_{02}^{(1)} = l_{02}^{(2)} = l_{02}^{(3)}$ has been suppressed for simplicity. Then, by substituting the mode parameters of Table 1 into Eq. (5) and setting the basic differential delay $\Delta\tau$ to 100 ps/km while keeping an incremental dispersion parameter as big as possible, we obtained the normalized lengths $l_{lm}^{(i)}$, as Table 2 shows. The position in which each LPG should be inscribed is obtained as the sum of the lengths along which the sample travelled on the different modes before arriving to that specific LPG. For instance, the third sample travels along the modes LP_{02}, LP_{12}, LP_{11} and LP_{31} passing through 3 LPGs placed in l_{02}, $l_{02} + l_{12}^{(3)}$, and $l_{02} + l_{12}^{(3)} + l_{11}^{(3)}$, respectively for LP_{02} to LP_{12}, LP_{12} to LP_{11} and LP_{11} to LP_{31} mode conversions. The equivalent sample group delays $\tau_{eq,\,i}$ - τ_{01} (normalized to the LP_{01} group delay) are 7882.3, 7982.3, 8082.3 and 8182.3 ps/km and the equivalent dispersions $D_{eq,i}$ are 12.1, 17.2, 22.3 and 27.4 ps/km/nm, respectively for samples 1 up to 4.

Table 2. Normalized lengths $l_{lm}^{(i)}$ along which the i-th sample travels on mode LP_{lm}.

l_{02}	$l_{12}^{(1)}$	$l_{41}^{(2)}$	$l_{01}^{(2)}$	$l_{12}^{(2)}$	$l_{31}^{(3)}$	$l_{11}^{(3)}$	$l_{12}^{(3)}$	$l_{21}^{(4)}$
0.17	0.83	0.24	0.22	0.37	0.39	0.26	0.18	1

Optics EXPRESS

The TTDL tunability is limited by the spectral bandwidth of the LPGs. From the effective indices of the fiber modes involved, we can calculate the period of each LPG Λ as, [17],

$$\Lambda = \frac{\lambda}{n_{eff_i} - n_{eff_j}}, \tag{6}$$

where $n_{eff,\,i}$ and $n_{eff,\,j}$ represent the effective indices of the involved modes. For the conversion between symmetrical and asymmetrical modes, we must inscribe the LPGs with a certain tilt angle to improve the mode conversion efficiency. We have recently demonstrated efficient symmetric-to-asymmetric and asymmetric-to-asymmetric mode conversions with tilted LPGs in a 4-LP-mode fiber, as well as symmetric-to-symmetric mode conversions without any tilt angle, [12,13]. Finally, we must note that the inscription of the LPGs with a certain chirp can provide up to a 20-nm wavelength operability range [18]. Table 3 summarizes the main characteristics of the designed LPGs.

Table 3. Calculated LPG periods and chirps for mode conversions and 20-nm tunability.

	LP_{02}-LP_{12}	LP_{12}-LP_{01}	LP_{01}-LP_{41}	LP_{12}-LP_{11}	LP_{11}-LP_{31}
Period (μm)	1057	233	217	264	404
Chirp (μm)	13	3	3	3	5
Normalized position	0.17	0.36	0.54	0.61	0.76

Figure 5 shows the computed differential group delay per unit length between the i^{th} and the first sample, $\tau_i - \tau_1$, $(i = 2, 3, 4)$, as a function of the optical wavelength λ. As shown, the basic differential group delay can be tuned from 49 ps/km at $\lambda = 1540$ nm up to 151 ps/km at $\lambda = 1560$ nm. We can observe as well a constant incremental value of the group delay slopes, that is, a constant incremental chromatic dispersion ΔD of 5.1 ps/km/nm. We must note that, up to a certain degree, this approach is robust against possible fiber fabrication deviations. Once the fiber is fabricated and its propagation characteristics are known (i.e., modal differential group delays and chromatic dispersions), we can modify the LPG positions to balance out possible group delays and chromatic dispersions mismatches between experimental and theoretical values.

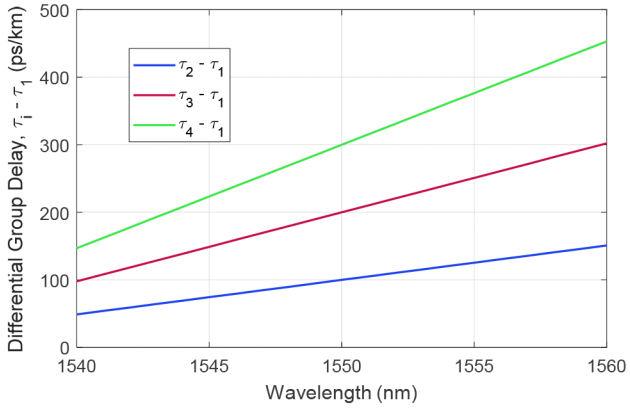

Fig. 5. Differential sample group delays per unit length with respect to the first sample as a function of the optical wavelength. TTDL tunability is ensured from 1540 up to 1560 nm.

4. Validation on microwave signal processing scenarios

We have evaluated theoretically the performance of the proposed tunable TTDL when it is applied to two typical MWP functionalities: tunable microwave signal filtering and optical beamforming

Optics EXPRESS

for phased array antennas. A microwave photonic signal filter can be implemented when we couple (interfere) together the four optical time-delayed signal samples at the ring-core fiber output before detecting them with a single photodetector, [19]. Following the same idea, we can implement a beamforming network for phased array antennas if each of the time-delayed signals at the output of the ring-core fiber is photodetected individually (instead of collectively) to feed a particular radiating element, [20].

Figure 6(a) shows the computed RF transfer function of the resulting microwave signal filter for different operation wavelengths and an RF frequency up to 50 GHz. We consider here a 1-km FMF link. Blue-dashed, orange-dashed and purple-solid lines correspond, respectively, to operation wavelengths of $\lambda = 1540.2$, 1550 and 1559.8 nm. We see that we can tune the Free Spectral Range (FSR) of the filter from 20 GHz down to 10 GHz and 6.67 GHz by changing the operation wavelength of the optical source from 1540.2 up to 1550 and 1559.8 nm, respectively. This corresponds to increasing the basic differential delay from 50 up to 100 and 150 ps, respectively. On the other hand, Fig. 6(b) depicts the simulated far-field radiation pattern (or array factor) of the resulting 4-element phased array antenna as a function of the beam angle (in degrees) for different basic differential delays for the same 1-km link. The distance between radiating elements is 1.5 cm and the RF frequency is set to 10 GHz. We see that we can tune the antenna beam-pointing angle by changing the operation wavelength with a tuning ratio of 5 degrees per nanometer. In particular, the beam-pointing angle varies from 36 down to 11 degrees by tuning the optical wavelength from 1543.7 up to 1547.7 nm.

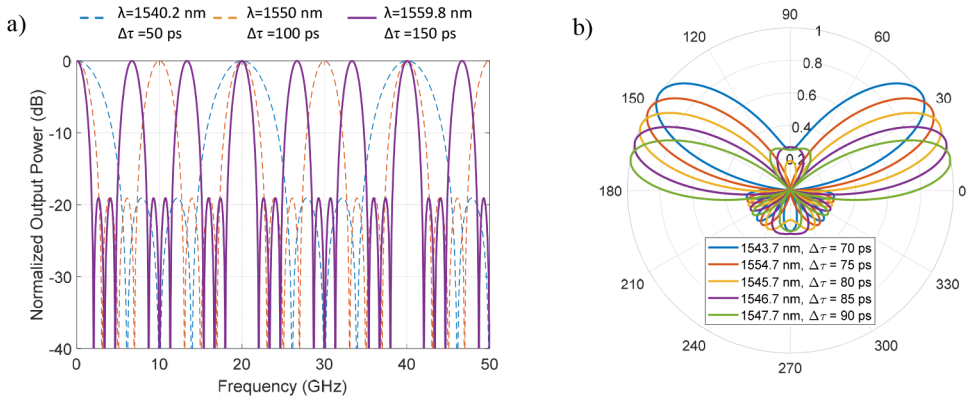

Fig. 6. (a) RF transfer function of the microwave photonic filter for three different operation wavelengths. (b) Array factor of the phased array antenna for five different operation wavelengths (RF frequency of 10 GHz and 1.5 cm antenna element separation).

5. Conclusions

Beyond high-capacity optical communications, SDM optical fibers can be exploited as a compact medium to implement "fiber-distributed signal processing" if they are engineered to operate as sampled TTDLs. One of the most desired features in this context relates to the capability to tune the basic differential delay of the TTDL with the optical wavelength linearly.

In summary, we have presented, for the first time to our knowledge, TTDL operation for RF signals over an FMF link exhibiting time delay tunability with the optical wavelength. We propose to achieve the required control over both the group delay and the chromatic dispersion of the signal samples by the custom design of a ring-core SI FMF where the inscription of a series of LPGs allows to excite higher-order modes at specific longitudinal locations along the fiber. In particular, we have designed a 4-sample TTDL approach that combines the design

Optics EXPRESS

of a 7-LP-mode ring-core fiber and the inscription of 5 LPGs at the appropriate longitudinal locations. This scheme requires to inject only the LP_{02} and LP_{21} modes into the fiber input while the 4 TTDL samples are given by the signals recovered from the LP_{21}, LP_{12}, LP_{31} and LP_{41} modes at the fiber output. A particular potential field of application can be found in fiber-wireless radio access networks where different functionalities can be implemented while transmitting the signal, for instance, between a central office and a given remote antenna. We have evaluated the performance of the designed tunable TTDL when it is applied to reconfigurable microwave signal filtering and radio beam-steering in phased array antennas.

The future experimental implementation of this concept requires, first, the actual fabrication of the ring-core fiber and the pertinent multiplexing/demultiplexing devices, what we consider feasible given the current state of SDM fabrication techniques. Second, we must bear in mind that the TTDL tunability range is subject to the optical bandwidth of the inscribed LPGs. Therefore, one has to ensure the LPGs are inscribed with the required grating periods and chirps to perform the proposed mode transformations along a 20-nm wavelength operability range.

Funding

European Research Council (Consolidator Grant 724663); Ministerio de Economía, Industria y Competitividad, Gobierno de España (BES-2015-073359 for S. García, RYC-2014-16247 for I. Gasulla, TEC2016-80150-R).

References

1. D. J. Richardson, J. M. Fini, and L. E. Nelson, "Space-division multiplexing in optical fibers," Nat. Photonics **7**(5), 354–362 (2013).
2. D. Barrera, I. Gasulla, and S. Sales, "Multipoint two-dimensional curvature optical fiber sensor based on a non-twisted homogeneous four-core fiber," J. Lightwave Technol. **33**(12), 2445–2450 (2015).
3. I. Gasulla and J. Capmany, "Microwave photonics applications of multicore fibers," IEEE Photonics J. **4**(3), 877–888 (2012).
4. J. Capmany, B. Ortega, D. Pastor, and S. Sales, "Discrete-time optical Processing of microwave signals," J. Lightwave Technol. **23**(2), 702–723 (2005).
5. W. Ng, A. A. Walston, G. L. Tangonan, J. J. Lee, I. L. Newberg, and N. Bernstein, "The first demonstration of an optically steered microwave phased array antenna using true-time-delay," J. Lightwave Technol. **9**(9), 1124–1131 (1991).
6. Z. Huet, J. Sun, L. Liu, and J. Wang, "All-optical tunable delay line based on wavelength conversion in semiconductor optical amplifiers and dispersion in dispersion-compensating fiber," Appl. Phys. A: Mater. Sci. Process. **91**(3), 421–428 (2008).
7. C. Wang and J. Yao, "Fiber Bragg gratings for microwave photonics subsystems," Opt. Express **21**(19), 22868–22884 (2013).
8. P. A. Morton and J. B. Khurgin, "Microwave photonic delay line with separate tuning of the optical carrier," IEEE Photonics Technol. Lett. **21**(22), 1686–1688 (2009).
9. J. Capmany, J. Mora, I. Gasulla, J. Sancho, J. Lloret, and S. Sales, "Microwave photonic signal processing," J. Lightwave Technol. **31**(4), 571–586 (2013).
10. I. Gasulla, D. Barrera, J. Hervás, and S. Sales, "Spatial division multiplexed microwave signal processing by selective grating inscription in homogeneous multicore fibers," Sci. Rep. **7**(1), 41727 (2017).
11. S. García and I. Gasulla, "Dispersion-engineered multicore fibers for distributed radiofrequency signal processing," Opt. Express **24**(18), 20641–20654 (2016).
12. R. Guillem, S. García, J. Madrigal, D. Barrera, and I. Gasulla, "Few-mode fiber true time delay lines for distributed radiofrequency signal processing," Opt. Express **26**(20), 25761–25768 (2018).
13. S. García, R. Guillem, J. Madrigal, D. Barrera, S. Sales, and I. Gasulla, "Sampled true time delay line operation by inscription of long period gratings in few-mode fibers," Opt. Express **27**(16), 22787–22793 (2019).
14. X. Zhao, Y. Liu, Z. Liu, Y. Zhao, T. Wang, L. Shen, and S. Chen, "Mode converter based on the long-period fiber gratings written in the two-mode fiber," Opt. Express **24**(6), 6186–6195 (2016).
15. D. Marcuse, "Derivation of Coupled Power Equations," Bell Syst. Tech. J. **51**(1), 229–237 (1972).
16. K. Ogawa, "Simplified theory of the multimode fiber coupler," Bell Syst. Tech. J. **56**(5), 729–745 (1977).
17. T. Erdogan, "Cladding-mode resonances in short- and long-period fiber grating filters," J. Opt. Soc. Am. A **14**(8), 1760–1773 (1997).
18. S. Ramachandran, J. Wagener, R. Espindola, and T. Strasser, "Effects of chirp in long period gratings," in Bragg Gratings, Photosensitivity, and Poling in Glass Waveguides **33**, Trends in Optics and Photonics Series, paper BE1 (1999).

Optics EXPRESS

19. J. Capmany, B. Ortega, and D. Pastor, "A Tutorial on Microwave Photonic Filters," J. Lightwave Technol. **24**(1), 201–229 (2006).
20. B. Ortega, J. Capmany, J. Cruz, M. V. Andrés, and D. Pastor, "Variable delay line for phased-array antenna based on a chirped fiber grating," IEEE Trans. Microwave Theory Tech. **48**(8), 1352–1360 (2000).